



 Cite this: *RSC Adv.*, 2022, 12, 25906

# Preparation and catalytic properties of polydopamine-modified polyacrylonitrile fibers functionalized with silver nanoparticles†

 Xiaoyu Zhu, Huiying Liu, \* Yingying Wu, Jing Ye, Yacheng Li and Zhendong Liu\*

Fiber-supported catalysts have attracted much attention due to their large specific surface area, high catalytic activity, and good recyclability. Functional polyacrylonitrile fibers were prepared by immersion of polyacrylonitrile fibers at room temperature in an alkaline dopamine (pH = 8.5) aqueous solution which can undergo self-polymerization and reduce silver ions to silver nanoparticles with mild reducibility and adsorption. The surface of the polyacrylonitrile fiber (PAN) was wrapped with a layer of polydopamine (PDA), and silver nanoparticles (Ag NPs) were adsorbed on the surface of PDA, forming an efficient fiber catalyst. The morphology and chemical composition of the catalyst material were characterized using scanning electron microscopy (SEM), X-ray diffraction (XRD) patterns, and Fourier transform infrared (FT-IR) and X-ray photoelectron spectroscopy (XPS). The catalytic activity of the nanocomposite was evaluated for the reduction reaction of 4-nitrophenol using sodium borohydride (NaBH<sub>4</sub>) at 35 °C with a material molar ratio of 1 : 10 and a fiber loaded catalysis dosage of 40 mg. The liquid phase yield can reach 98% in 30 minutes and can be reused after washing with ethanol. Moreover, the composite material exhibited a good stability up to 10 cycles without a significant loss of its catalytic activity. The results show that the catalyst is easy to recover from the reaction system and has maintained good stability and catalytic activity after many cycles.

 Received 22nd June 2022  
 Accepted 17th August 2022

DOI: 10.1039/d2ra03845e

[rsc.li/rsc-advances](https://rsc.li/rsc-advances)

## Introduction

Silver nanocatalysts have low price, antibacterial activity and very stable physical and chemical properties, so they are widely used in optics,<sup>1,2</sup> catalysis,<sup>3–6</sup> antibacterial<sup>7,8</sup> and other fields.<sup>9,10</sup> Many methods have been reported to synthesize silver nanomaterials, such as the gas condensation method,<sup>11</sup> localized surface plasmon resonance,<sup>12</sup> mechanical grinding,<sup>13</sup> irradiation<sup>14</sup> and the microwave method,<sup>15</sup> but these methods generally require harsh conditions, low pressure inert gas or specialized equipment. The chemical reduction method<sup>16</sup> has been widely used due to the advantages of simple experimental conditions, low cost, and easy control. Commonly used reducing agents in chemical reduction methods are sodium borohydride, formaldehyde, *etc.*, and silver nitrate is used as the silver source.<sup>17</sup>

Polydopamine (PDA) is a bio-macromolecule formed by polymerization of phenolic compounds, which not only has strong adhesiveness to various surfaces, but also has high adsorption ability to metal ions.<sup>18</sup> In addition, PDA can be used as a mild reducing agent to reduce Ag<sup>+</sup> on different matrices.<sup>19</sup> It

is also found that the O- and N-atoms in PDA can chelate with Ag nanoparticles (AgNPs) to improve their durability. The PDA coatings have great potential in smart materials,<sup>20</sup> biomedical field<sup>21</sup> and carrier of catalysis.<sup>22</sup>

Polyacrylonitrile (PAN) fibers have low-cost, large surface areas, close structure, high mechanical strength, good acid resistance and oxidation resistance, widely used in industry and our daily life. Besides, PAN fibers are abundant of nitrile groups which can be easily converted into other groups<sup>23,24</sup> like carboxyl, amide, amidoxime, *etc.* Furthermore, it can be employed as polymer fiber-carriers extracted from the reaction system by simple filtration or woven into fabrics served in continuous flow of fluid.<sup>25</sup> Herein, the PAN fiber catalyst loaded with Ag nanoparticles was prepared by reducing the silver ions to silver nanoparticles on the fiber surface by using the adhesive and reductive properties of polydopamine.

## Experimental

### Materials and methods

PAN fibers were obtained from Jilin Chemical Fiber Factory. Dilute sulfuric acid (H<sub>2</sub>SO<sub>4</sub>), absolute ethanol (C<sub>2</sub>H<sub>5</sub>OH), dopamine hydrochloride, Tris-HCl buffer, AgNO<sub>3</sub> (analytically pure), *p*-nitrophenol were purchased from Beijing Chemical Plant and used without further purification. Sodium borohydride (NaBH<sub>4</sub>) were obtained from Adamas Reagent.

School of Material Design and Engineering, Beijing Institute of Fashion Technology, Beijing 100029, P. R. China. E-mail: 20140006@bift.edu.cn; clyzd@bift.edu.cn

† Electronic supplementary information (ESI) available. See <https://doi.org/10.1039/d2ra03845e>



Fiber morphologies were observed using a scanning electron microscopy (SEM, JEOL JSM-7500F) under an accelerating voltage of 5 kV. The chemical structure of the fibers was analyzed using Fourier transform infrared (FT-IR, PerkinElmer) spectroscopy. The precise Ag loading of functionalized fibers was tested by Inductively Coupled Plasma Mass Spectrometry (Agilent ICPOES730). The thermal stability of fibers was investigated by thermogravimetric analysis (TG, NSK Ltd.) under nitrogen atmosphere, and the heating rate was controlled as  $10\text{ }^{\circ}\text{C min}^{-1}$ . The X-ray powder diffraction (XRD) profiles of the fibers were studied *via* a X-ray diffractometer (Oxford) in the range of  $10$  and  $90^{\circ}$  using a Vantec-1 position sensitive detector and the step size was set as  $0.01^{\circ}$ . Chemical composition analysis of samples was evaluated by an X-ray photoelectron spectrometer (XPS, Thermo Fisher 250Xi). The reaction was analyzed by high-performance liquid chromatography (Shimadzu, LC-20AT) and UV-vis spectrophotometry (TU-1810) at wavelengths of 250 to 500 nm.

### Preparation of functional fibers

Polyacrylonitrile fibers functionalized with silver nanoparticles *via* polydopamine (PDA) was prepared according to ref. 26. The original PAN fibers were firstly soaked in sulfuric acid (30 wt%) under ultrasonic treatment for half an hour, which was then heated at  $110\text{ }^{\circ}\text{C}$  for 2 h for sulfonation. To remove the residual reactants, the modified fibers were rinsed with distilled water. After vacuum drying at  $70\text{ }^{\circ}\text{C}$  for 4 h, the fibers were collected and named as sulfonated PAN (PAN-S) fibers. Dopamine hydrochloride aqueous solution of pH 8.5 is prepared by adding Tris-HCl (1 L) into 1 g dopamine hydrochloride aqueous solution. Polydopamine functionalized PAN (PAN-S-PDA) was obtained through immersion of the PAN-S into the dopamine solution for 12 h at  $30\text{ }^{\circ}\text{C}$ , followed by rinsing with water. AgNPs deposition was achieved through a simple immersion of PAN-PDA in  $1\text{ g L}^{-1}$  ( $2\text{ g L}^{-1}$ ,  $3\text{ g L}^{-1}$ ,  $4\text{ g L}^{-1}$ )  $\text{AgNO}_3$  aqueous solution for 12 h at  $30\text{ }^{\circ}\text{C}$ . The morphology and structure of polyacrylonitrile fibers with a load of 1.6% were characterized by SEM, Fourier infrared spectroscopy, Ultraviolet visible absorption spectroscopy, X-ray diffraction and thermal gravity.

### Catalytic reduction of 4-nitrophenol

The catalytic reduction of 4-nitrophenol (4-NP) was carried out at  $35\text{ }^{\circ}\text{C}$  in a round-bottom flask containing 0.139 g (1 mmol) of 4-nitrophenol, 0.378 g (10 mmol) of  $\text{NaBH}_4$  and 40 mg of PAN-PDA-Ag mixed. 4-NP was added to the reaction bottle containing  $\text{NaBH}_4$  and the initial pale yellow color changed to colorless as the reaction progressed due to the formation of 4-aminophenol (4-AP). The reaction progress was monitored by liquid chromatography.

## Results and discussion

### Morphological characterization of PAN-S-PDA-Ag fibers

Fig. 1(a–f) shows the morphological changes of polyacrylonitrile fibers before and after modification. It can be seen from the figure that the surface of the original fiber is smooth, the

structure is dense and uniform, and the longitudinal grooves are very shallow. In order to improve the hydrophilicity of the fiber, the polyacrylonitrile fiber is sulfonated with dilute sulfuric acid. The surface structure is destroyed and the surface morphology becomes rough. To make dopamine stick firmly to the PAN fibers, the PAN fibers were calcined in an oven at  $200\text{ }^{\circ}\text{C}$  until the fibers turned from white to orange. After pre-oxidation, the longitudinal grooves were deepened and the surface morphology rougher. There is a sort of thin and dense dopamine coating, which can self-polymerize into polydopamine and reduce silver ion into nanoparticles adhered to the surface of the PAN fibers. PDA was wrapped on the surface of PAN to form a core-shell like functionalized fiber (Fig. S1†), and the amount of PDA on PAN fiber increased with the increase of PDA concentration, which played an important role in the subsequent silver loading and catalytic performance (Table S1†). Silver nanoparticles with a diameter of about 100 nm can be uniformly distributed without obvious agglomeration.

### Structural characterization of PAN-S-PAD-Ag fibers

Fig. 2 shows the FT-IR spectra of polyacrylonitrile fibers before and after modification. There is a strong absorption peak at  $2238\text{ cm}^{-1}$ , which is the stretching vibration of  $-\text{C}\equiv\text{N}$ .  $2926\text{ cm}^{-1}$  is the stretching vibration of the methylene group. The  $\text{C}=\text{O}$  stretching bond frequency of the ester carbonyl group of the second monomer is absorbed at  $1733\text{ cm}^{-1}$ . Strong  $\text{C}=\text{O}$  asymmetric stretching bonding frequencies can be observed at  $1500\text{ cm}^{-1}$ , overlapping with  $\text{N}-\text{H}$  deformation and  $\text{C}-\text{N}$  stretching vibrations. The results showed that the degradation during acid treatment and pre-oxidation resulted in the formation of unsaturated  $\text{C}=\text{C}$  double bonds, and no significant changes were detected after dopamine-functionalized loading of silver nanoparticles.

To find the ideal pre-oxidation temperature, the thermal degradation behavior of the fibers under air atmosphere was evaluated using thermogravimetric analysis (TG). As can be seen from Fig. 3 and Table 1, the main degradation is between  $250\text{ }^{\circ}\text{C}$  and  $480\text{ }^{\circ}\text{C}$ . To avoid severe degradation, pre-oxidation temperature below  $250\text{ }^{\circ}\text{C}$  should be selected. In this experiment,  $200\text{ }^{\circ}\text{C}$  was chosen as the pre-oxidation temperature. It is worth mentioning that the residual weight of PAN-S (44%) at

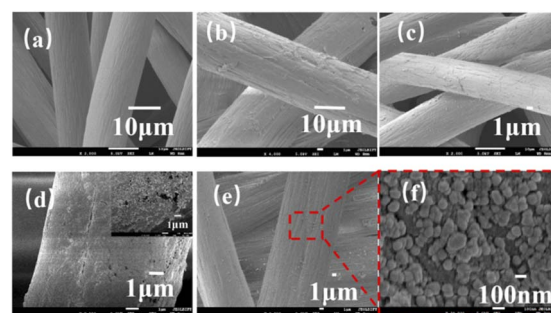


Fig. 1 The SEM images of (a) PAN (b) PAN- $\text{H}_2\text{SO}_4$  (c) PAN-S fiber (d) PAN-S-PDA fiber, the insert is the surface of PAN-S-PDA fiber (e) PAN-S-PDA-Ag fiber (f) the local amplification of PAN-S-PDA-Ag fiber.

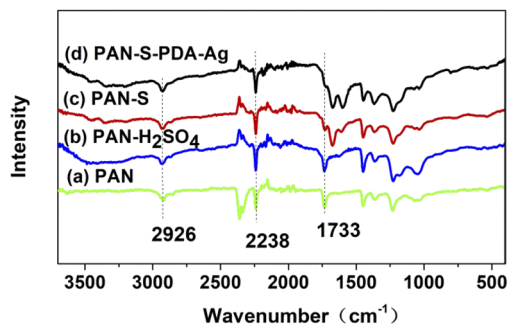


Fig. 2 The FTIR spectra of (a) PAN (b) PAN-H<sub>2</sub>SO<sub>4</sub> (c) PAN-S (d) PAN-S-PDA-Ag.

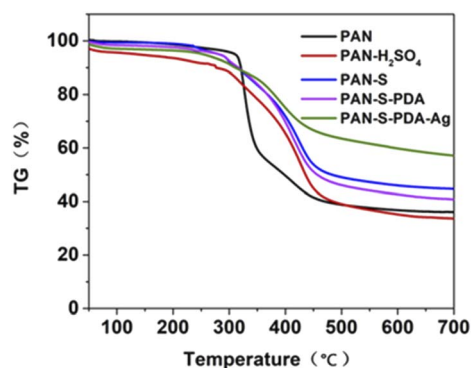


Fig. 3 Thermal gravimetry analysis of PAN, PAN-H<sub>2</sub>SO<sub>4</sub>, PAN-S, PAN-S-PDA, PAN-S-PDA-Ag fibers.

700 °C is much higher than that of untreated PAN (35%) at 700 °C, indicating that pretreatment can lead to structural changes and enhancing the thermal stability. Therefore, the preprocessing strategy facilitates functionalization.

The composition and phase structure of the synthetic product were analyzed by XRD. Fig. 4 depicts the XRD pattern of PAN and silver nanoparticles modified fibers. The sample used for XRD analysis was a silver nanoparticle with an average particle size of 100 nm. Because the high molecular strands in PAN are concentrated closely, a certain crystalline region is formed. The molecular arrangement in the crystalline region makes it difficult for other small molecules to enter the crystalline region, so there is a distinct peak at  $2\theta = 17^\circ$ . The  $2\theta$  angle shows a wide diffuse reflection region between  $17 \sim 30^\circ$

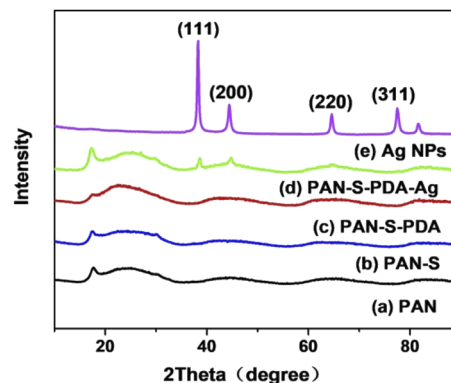


Fig. 4 XRD pattern of (a) PAN, (b) PAN-S, (c) PAN-S-PDA, (d) PAN-S-PDA-Ag, (e) Ag NPs.

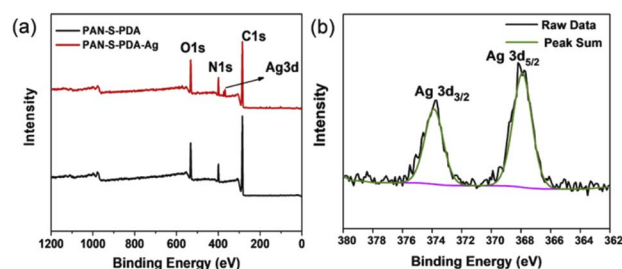


Fig. 5 (a) X-ray photoelectron spectroscopy of full spectrum of PAN-S-PDA and PAN-S-PDA-Ag (b) XPS narrow spectrum of Ag3d.

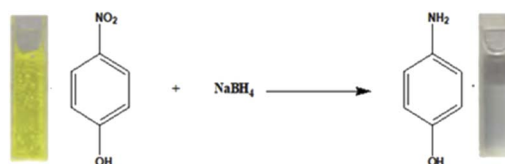


Fig. 6 Reaction of sodium borohydride reduction of nitrophenol.

because of the disordered phase in the structure. In addition, there are four distinct peaks in the figure at  $38.6^\circ$ ,  $44.9^\circ$ ,  $64.8^\circ$  and  $77.8^\circ$ . These four peaks agree well to the (111), (200), (220) and (311) crystalline surfaces of the face-to-face cubic phase of Ag (Fig. 4d and 4e). It can be judged that silver nanoparticles were prepared successfully.

Table 1 Thermal gravimetric analysis of PAN, PAN-H<sub>2</sub>SO<sub>4</sub>, PAN-S, PAN-S-PDA, PAN-S-PDA-Ag fibers

Sample	Quality loss process indicators (°C)			
	Temperature of initial decomposition	Maximum decomposition rate temperature	Termination decomposition temperature	Residual mass at 700 °C (%)
PAN	312	336	445	35
PAN-H <sub>2</sub> SO <sub>4</sub>	280	430	480	33
PAN-S	280	430	452	44
PAN-S-PDA	280	392	458	41
PAN-S-PDA-Ag	250	415	462	57

Table 2 Reaction activity of sodium borohydride reduced 4-NP catalyzed by fibers with different nano-silver loads

Silver load	$n_{4\text{-NP}} : n_{\text{NaBH}_4}$	Amount of cat. (mg)	Solvent	$T$ ( $^{\circ}\text{C}$ )	$t$ (min)	Yield (%)
0.32%	1 : 10	40	H <sub>2</sub> O	35	24 min	97
0.68%	1 : 10	40	H <sub>2</sub> O	35	17 min	97
1.57%	1 : 10	40	H <sub>2</sub> O	35	16 min	97
2.20%	1 : 10	40	H <sub>2</sub> O	35	19 min	98

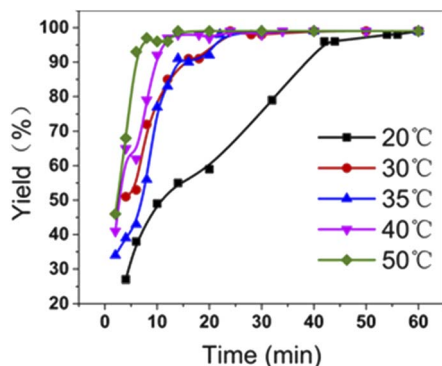
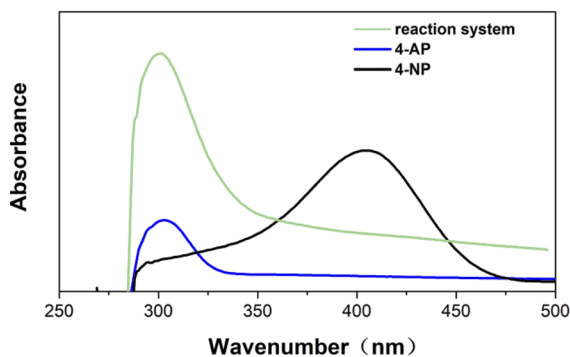
Fig. 7 Liquid phase yield diagram of the reaction at different temperatures (■) 20  $^{\circ}\text{C}$ ; (●) 30  $^{\circ}\text{C}$ ; (▲) 35  $^{\circ}\text{C}$ ; (▼) 40  $^{\circ}\text{C}$ ; (◆) 50  $^{\circ}\text{C}$ .

Fig. 8 UV-Vis absorption spectrum of raw material 4-NP, 4-AP standard sample and reaction system after 30 minutes.

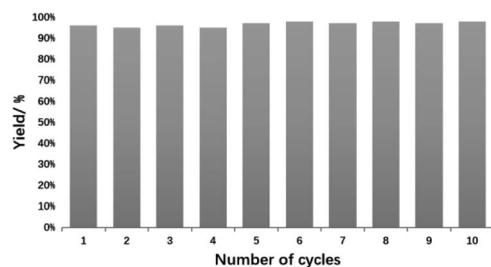


Fig. 9 Reuse of fibers.

The Fig. 5a shows the XPS full spectrum of PAN-S-PDA and PAN-S-PDA-Ag. It can be seen that the fibers without Ag NPs are composed of C, N, and O elements, whose characteristic peaks

located at 248.4 eV, 399.4 eV and 531.9 eV, respectively. The fiber loaded with Ag NPs has an additional Ag peak at 367.9 eV, indicating that the silver nanoparticles were successfully loaded on the dopamine-modified polyacrylonitrile fiber. Fig. 5b exhibits the XPS narrow spectrum of Ag3d, which can be well fitted into peaks at 367.9 eV (Ag3d<sub>5/2</sub>), and 373.9 eV (Ag3d<sub>3/2</sub>). Silver was confirmed to be attached to functional fibers in a zero-valence form.

### Study on catalytic performance of PAN-S-PDA-Ag

Functional polyacrylonitrile fiber with different amount of silver loading was obtained by adjusting the concentration of AgNO<sub>3</sub>. The functional fibers were used to catalyze the reduction reaction of 4-nitrophenol (4-NP), see Fig. 6. The reactant 4-NP (1 mmol), reducing agent sodium borohydride 0.378 g (10 mmol) and catalyst 40 mg PAN-PDA-Ag were used and reacted at 35  $^{\circ}\text{C}$ . Upon adding 4-NP to the reaction bottle containing NaBH<sub>4</sub>, the solution becomes yellow-green. When the 4-NP is fully converted to the product 4-aminophenol (4-AP), the solution becomes colorless, and the progress of the reaction is monitored by liquid chromatography. When the silver loading increased from 0.32% to 0.68%, the reaction time decreased from 24 minutes to 17 minutes, with the reaction yield more than 97% (Table 2). The concentration of silver nitrite further increased, the loading of silver rose but the catalytic efficiency of 4-nitrophenol was not increased obviously. So the fiber with a load of 0.68% was selected to characterize its morphology and structure, as well as do the recycle fiber catalyst for reaction.

The effects of temperature and fiber dosage on 4-NP reduction were investigated. As can be seen in Fig. 7, the reaction takes 40 minutes to complete at 20  $^{\circ}\text{C}$ , but at 50  $^{\circ}\text{C}$  it takes only eight minutes to get 97% yield, so it is found that at 20 ~ 50  $^{\circ}\text{C}$ , the faster the catalytic reaction proceeds as the temperature rises. In addition, no obvious change was detected when the amount of PAN-S-PDA-Ag was less than 15 mg. As the amount of fiber was between 30 mg and 40 mg, the liquid-phase yield of the reaction could reach 99% within 1 h (Table S2†).

In order to clarify the mechanism of functionalized fiber catalysis, the control experiments of four different catalyst compositions were conducted (Table S3†). It is found that the reduction of *p*-nitrophenol (4-NP) to *p*-aminophenol (4-AP) can be catalyzed within 30 minutes when Ag and NaBH<sub>4</sub> are working together as catalyst, neither Ag nor NaBH<sub>4</sub> can work when using as catalyst alone. Based on the above experimental data and theoretical analysis, it is confirmed that the role of polyacrylonitrile (PAN) in functionalized fibers acts as a carrier. It is convenient to recycle after the reaction of the catalytic system.



The role of PDA acts not only as a bridge for loading silver nanoparticles onto polyacrylonitrile fibers, but also as a reducing agent for reducing silver ions to silver. The catalytic mechanism of *p*-nitrophenol catalyzed by poly-acrylonitrile fibers loaded with nano-silver is proposed: the silver nanoparticles can adsorb  $\text{NaBH}_4$  and 4-NP molecules, and the electrons are transferred rapidly from  $\text{BH}_4$  to 4-NP *via* the surface of the silver nanoparticles during the reaction. The rapid transfer of electrons can increase the potential difference and further promote the transfer of electrons from  $\text{BH}_4$  to 4-NP, thus making the functional fibers have superior catalytic properties.

Fig. 8 shows UV-Vis absorption spectra of raw material 4-NP, 4-AP standard sample and reaction system after 30 minutes. The 4-NP standard has an absorption maximum at 400 nm, and the 4-AP standard has an absorption maximum at 303 nm. After 30 minutes of reaction system, a peak appeared at 300 nm, and the peak at 400 nm almost disappeared, indicating that 4-nitrophenol catalyzed by PAN-S-PDA-Ag was almost completely reduced to 4-AP. The PAN-S-PDA-Ag showed good stability for up to 10 cycles after ethanol washing without significant loss of catalytic activity (Fig. 9 and Table S4<sup>†</sup>). The SEM images (Fig. S2<sup>†</sup>) show lots of silver nanoparticles are still uniformly attached to the surface of the fiber catalysts after ten times of use. So the functionalized catalysts still maintain high catalytic performance.

## Conclusions

Using polydopamine as adhesive and reducing agent, the nano-silver catalyst loaded polyacrylonitrile fiber was successfully prepared by simple impregnation method. The catalyst can reduce 4-NP at 35 °C with high catalytic activity and be easily regenerated. PAN-S-PDA-Ag catalyst could reuse 10 times after ethanol washing, and the catalytic activity has not decreased significantly. The high catalytic activity and outstanding recoverability of PAN-S-PDA-Ag provide a more environmentally friendly, safe and economical choice for reducing nitrophenol compounds, which is expected to a big contribution to environmental protection.

## Author contributions

Huiying Liu: conceptualization, funding acquisition, methodology, resources, writing–review & editing. Xiaoyu Zhu: data curation, writing–original draft. Yingying Wu: data curation. Jing Ye: data curation. Yacheng Li: investigation. Zhendong Liu: investigation, visualization, review.

## Conflicts of interest

There are no conflicts to declare.

## Acknowledgements

This work was supported by National Natural Science Foundation of China (No. 21603008), 2022 Graduate Research and Innovation Project of Beijing Institute of Fashion Technology

(grant no. X2022-046), and Key Young Teachers Program of Beijing Institute of Fashion Technology (grant no. BIFTQG202003).

## Notes and references

- 1 I. Shutsko, C. M. Böttge, J. v. Barga, A. Henkel, M. Meudt and P. Görrn, Enhanced hybrid optics by growing silver nanoparticles at local intensity hot spots, *Nanophotonics*, 2019, **8**, 1457–1464.
- 2 S. Pugazhendhi, E. Kirubha, P. K. Palanisamy and R. Gopalakrishnan, Synthesis and characterization of silver nanoparticles from *Alpinia calcarata* by Green approach and its applications in bactericidal and nonlinear optics, *Appl. Surf. Sci.*, 2015, **357**, 1801–1808.
- 3 X. Chen, Y. Li, X. Pan, D. Cortie, X. Huang and Z. Yi, Photocatalytic oxidation of methane over silver decorated zinc oxide nanocatalysts, *Nat. Commun.*, 2016, **7**, 12273–12280.
- 4 H. Wang, G. Zhang, R. Mia, W. Wang, L. Xie, S. Lü, S. Mahmud and H. Liu, Bioreduction ( $\text{Ag}^+$  to  $\text{Ag}^0$ ) and stabilization of silver nanocatalyst using hyaluronate biopolymer for azo-contaminated wastewater treatment, *J. Alloys Compd.*, 2022, **894**, 162502–162513.
- 5 H. Veisi, N. Dadres, P. Mohammadi and S. Hemmati, Green synthesis of silver nanoparticles based on oil-water interface method with essential oil of orange peel and its application as nanocatalyst for A3 coupling, *Mater. Sci. Eng. C*, 2019, **105**, 110031–110051.
- 6 X. Wu, F. Chen, N. Zhang, Y. Lei, Y. Jin, A. Qaseem and R. L. Johnston, Activity Trends of Binary Silver Alloy Nanocatalysts for Oxygen Reduction Reaction in Alkaline Media, *Small*, 2017, **13**, 1603387–1603394.
- 7 M. Riaz, U. Sharafat, N. Zahid, M. Ismail, J. Park, B. Ahmad, N. Rashid, M. Fahim, M. Imran and A. Tabassum, Synthesis of Biogenic Silver Nanocatalyst and their Antibacterial and Organic Pollutants Reduction Ability, *ACS Omega*, 2022, **7**, 14723–14734.
- 8 S. Tang and J. Zheng, Antibacterial Activity of Silver Nanoparticles: Structural Effects, *Adv. Healthcare Mater.*, 2018, **7**, 1701503–1701512.
- 9 X. Zhang, S. Yang, B. Yu, Q. Tan, X. Zhang and H. Cong, Advanced Modified Polyacrylonitrile Membrane with Enhanced Adsorption Property for Heavy Metal Ions, *Sci. Rep.*, 2018, **8**, 1260–1268.
- 10 P. Kampalanonwat and P. Supaphol, Preparation of Hydrolyzed Electrospun Polyacrylonitrile Fiber Mats as Chelating Substrates: A Case Study on Copper(II) Ions, *Ind. Eng. Chem. Res.*, 2011, **50**, 11912–11921.
- 11 M. Raffi, A. K. Rumaiz, M. M. Hasan and S. I. Shah, Studies of the growth parameters for silver nanoparticle synthesis by inert gas condensation, *J. Mater. Res.*, 2007, **22**, 3378–3384.
- 12 T. Hong, A. Lu, W. Liu and C. Chen, Microdroplet Synthesis of Silver Nanoparticles with Controlled Sizes, *Micromachines*, 2019, **10**, 274–283.
- 13 M. Baláž, Z. Bedlovičová, N. Daneu, P. Siksa, L. Sokoli, Ľ. Tkáčiková, A. Salayová, R. Džunda, M. Kováčová,

- R. Bureš and Z. L. Bujňáková, Mechanochemistry as an Alternative Method of Green Synthesis of Silver Nanoparticles with Antibacterial Activity: A Comparative Study, *Nanomaterials*, 2021, **11**, 1139–1163.
- 14 K. Wang, Z. Liu, T. Zhang, Y. Qin and X. Yang, Structural transition of synthesized silver nanoparticles under irradiation, *Colloids Surf., A*, 2019, **570**, 89–95.
- 15 P. E. J. Saloga, C. Kästner and A. F. Thünemann, High-Speed but Not Magic: Microwave-Assisted Synthesis of Ultra-Small Silver Nanoparticles, *Langmuir*, 2018, **34**, 147–153.
- 16 H. S. Bahlol, M. F. Foda, J. Ma and H. Han, Robust Synthesis of Size-Dispersal Triangular Silver Nanoprisms via Chemical Reduction Route and Their Cytotoxicity, *Nanomaterials*, 2019, **9**, 674–687.
- 17 S. Halder, A. N. Ahmed, M. A. Gafur, G. Seong and M. Z. Hossain, Size-Controlled Facile Synthesis of Silver Nanoparticles by Chemical Reduction Method and Analysis of Their Antibacterial Performance, *ChemistrySelect*, 2021, **6**, 9714–9720.
- 18 K. R. Kim, J. Kim, J. W. Kim, C. T. Yavuz, M. Y. Yang and Y. S. Nam, Light-activated polydopamine coatings for efficient metal recovery from electronic waste, *Sep. Purif. Technol.*, 2021, **254**, 117674–117686.
- 19 Y. Liu, H. Zhou, J. Wang, D. Yu, Z. Li and R. Liu, Facile synthesis of silver nanocatalyst decorated Fe<sub>3</sub>O<sub>4</sub>@PDA core-shell nanoparticles with enhanced catalytic properties and selectivity, *RSC Adv.*, 2022, **12**, 3847–3855.
- 20 P. Yang, F. Zhu, Z. Zhang, Y. Cheng, Z. Wang and Y. Li, Stimuli-responsive polydopamine-based smart materials, *Chem. Soc. Rev.*, 2021, **50**, 8319–8343.
- 21 I. S. Kwon and C. J. Bettinger, Polydopamine nanostructures as biomaterials for medical applications, *J. Mater. Chem. B*, 2018, **6**, 6895–6903.
- 22 Z. Wang, Y. Zou, Y. Li and Y. Cheng, Polydopamine Nanomaterials: Metal-Containing Polydopamine Nanomaterials: Catalysis, Energy, and Theranostics, *Small*, 2020, **16**, 1907042–1907062.
- 23 G. Li, J. Xiao and W. Zhang, Knoevenagel condensation catalyzed by a tertiary-amine functionalized polyacrylonitrile fiber, *Green Chem.*, 2011, **13**, 1828–1836.
- 24 G. Xu, L. Wang, Y. Xie, M. Tao and W. Zhang, Highly selective and efficient adsorption of Hg<sup>2+</sup> by a recyclable aminophosphonic acid functionalized polyacrylonitrile fiber, *J. Hazard. Mater.*, 2018, **344**, 679–688.
- 25 G. Xu, Y. Zhao, L. Hou, J. Cao, M. Tao and W. Zhang, A recyclable phosphonic acid functionalized polyacrylonitrile fiber for selective and efficient removal of Hg<sup>2+</sup>, *Chem. Eng. J.*, 2017, **325**, 533–543.
- 26 Q. Yang, X. Guo, X. Ye, H. Zhu, L. Kong and T. Hou, Functionalized polyacrylonitrile fibers with durable antibacterial activity and superior Cu(II)-removal performance, *Mater. Chem. Phys.*, 2020, **245**, 122755.